CrossMark

RESEARCH PAPER

The use of polybutene for controlling the flow of liquids in centrifugal microfluidic systems

Salar Soroori[1] · José Manuel Rodriguez-Delgado[4] · Horacio Kido[2,3] · Graciano Dieck-Assad[4] · Marc Madou[1,2,5] · Lawrence Kulinsky[2]

Abstract The field of centrifugal microfluidics has evolved over the last several decades to allow implementation of complex biological and chemical assays on Lab-on-Disc (LOD) platforms. Present study describes the use of polymer polybutene for tuning hydrophobic siphons and for liquid volume definition on a centrifugal microfluidic platform. Both the siphon tuning and the volume definition steps are carried out by generating negative pressure that results from the volume expansion caused by the transfer of polybutene from a dedicated chamber into a secondary reservoir via a connecting siphon. The hydrophobic valve of the chamber that holds polybutene bursts open at specific angular velocities that depend on the height and density of the liquid column. Thus, the parameters of siphon activation can be adjusted by tuning the burst angular velocity of the valve that is driven by filling the tuning reservoir with a specific volume of polybutene. The same disc construction can be utilized to provide volume definition functionality to transfer liquids from one reservoir to another reservoir in as many fractions as there are immiscible liquids of different densities in the tuning chamber. The presented work also demonstrates the use of polybutene in sealing fluidic chambers to improve heating efficiency and to minimize evaporation during thermal cycling required for applications such as PCR amplification. Finally, the use of polybutene as a stationary liquid phase in droplet production on a spinning disc is demonstrated.

Keywords Viscoelastic material · Polybutene · Centrifugal microfluidics · Hydrophobic siphon · Tuning valve · Volume definition · Liquid polymer

✉ Salar Soroori
 ssoroori@uci.edu

1 Department of Biomedical Engineering, University of California, Irvine, CA 92697, USA

2 Department of Mechanical & Aerospace Engineering, University of California, Irvine, CA 92697, USA

3 RotaPrep, Inc., Tustin, CA 92782, USA

4 Sensors and Devices Research Group, School of Engineering and Sciences, Tecnológico de Monterrey, Monterrey, Mexico

5 UNIST, World Class University (WCU), Ulsan, South Korea

1 Introduction

The technical advances of the last decade in the field of centrifugal microfluidics have allowed development of portable desktop "Lab-on-a-disc" (also known as "Lab-on-CD") platforms capable of performing biological or chemical assays as an alternative to conventional laboratory tests. The ultimate goal for developing such devices is to make sample-to-answer microfluidic platforms that can execute a completely automated sequence of integrated steps from sample introduction and processing to PCR amplification and detection of results (Gorkin et al. 2010; Strohmeier et al. 2015). In order to achieve the required integration and automation, many fluidic processes such as sample lysis and clarification, valving, mixing, volume definition, DNA amplification via PCR (Madou et al. 2006; Ducree et al. 2007; Aeinehvand et al. 2015), and detection techniques such as optical, fluorescence, and electrochemical methods have been realized on microfluidic discs (Imaad et al. 2011; Steigert et al. 2006; Sundberg et al. 2010; Kim et al. 2011).

Fluidic valving is a critical step that controls passage of liquid from one reservoir to another. Valving techniques employed on microfluidic discs can be categorized into either "passive" or "active." Passive valves do not need any external equipment for operation and are based on the interplay between capillary and centrifugal forces. Depending on whether the channels are hydrophilic or hydrophobic, the centrifugal force acts either to impede the liquid motion (for hydrophilic channels) or to burst through restraining forces (for hydrophobic channels) (Madou et al. 2006). In hydrophobic channels, liquid does not advance until the centrifugal force overcomes the liquid surface tension. Therefore, such valves are "normally closed," and more robust operation (as compared to hydrophilic valves) is achievable since no spontaneous liquid movement occurs (Abi-Samra et al. 2011a). Additionally, many plastics are natively hydrophobic; thus, the need and cost of surface treatment to modify the contact angle are avoided (Beaulieu et al. 2009; Gorkin et al. 2011). Passive hydrophobic valves are made either by an abrupt constriction within a hydrophobic channel or by placing a patch of a hydrophobic coating within a hydrophilic channel that prevents liquid from moving past that hydrophobic zone (Gorkin et al. 2010; Madou et al. 2006). Some of the new developments for "passive" valving include timed liquid valving and pumping (Schwemmer et al. 2015) that can accurately control the release of fluid within a time period in a passive manner and passive liquid valve (PLV) that is based on utilizing venting chambers and the effect of pressure equilibrium on microfluidic discs (Al-Faqheri et al. 2015). Passive valves are generally not vapor tight and hence are inappropriate for long-term liquid and reagent storage on discs or for preventing liquid loss due to evaporation (Abi-Samra et al. 2011b). Because of the manufacturing imperfections of typical fabrication processes (such as milling), it is difficult to precisely control the burst angular velocity of passive valves (Thio et al. 2013). In order to address these problems, "active" valves, such as wax valves and ice valves, have been developed for microfluidic discs (Park et al. 2007; Amasia 2011; Abi-Samra et al. 2011b). Active pneumatic control of fluid flow (Clime et al. 2015) and solvent-selective routing (Dimov et al. 2014) are some of the recent additions to available "active" valving techniques. These active valves are vapor-tight, and they provide on-demand valving (as compared to passive valves), albeit at the expense of the need for additional peripheral equipment such as lasers and IR lamps. Recently, several groups have demonstrated vapor-tight passive valves that utilize dissolvable films (Gorkin et al. 2012a, b) and metalized plastic pouches that burst open when the angular velocity of a disc exceeds a critical value (van Oordt et al. 2013). Another recently developed valve is based on using negative pressure (vacuum) that is generated inside a radial channel as

liquid inside that channel exits into a connecting reservoir (Gorkin et al. 2011). This vacuum can be employed to move liquid out of an adjoining reservoir via a hydrophobic siphon. This work presents a method to control the activation of such a hydrophobic siphon at different rotational angular velocities without the need to change the geometric position of the siphon with respect to the disc center. This "tunable" type of hydrophobic siphon can also assist in assaying a specific predetermined volume of reagents or samples.

Many biological assays require DNA amplification of a sample prior to detection. DNA amplification has been demonstrated on microfluidic discs (Amasia et al. 2012; Sundberg et al. 2010; Oh et al. 2015; Czilwik et al. 2015a). Evaporative loss is a common problem related to thermal cycling required for PCR amplification. Undesired evaporation becomes even more pronounced in microfluidic platforms since the liquid volume is very small (typically in the order of microliters). Sealing of fluidic chambers on microfluidic discs has been demonstrated by the use of ice valves as a solution to minimize the evaporative loss of liquid during PCR amplification (Amasia 2011). Mineral oil (Wang et al. 2013) has also been demonstrated to minimize the loss of liquid due to evaporation. Also Czilwik et al. (2015b) have demonstrated that evaporation loss during thermal cycling can be significantly reduced by using vapor diffusion barriers. The fluidic design presented in this work relies on polybutene for sealing the sample undergoing thermal cycling. This sealing method decreases evaporation and increases the heating rate. It does not require peripheral equipment for activation.

Droplet generation is yet another area of microfluidic research that is rapidly growing in importance (Teh et al. 2008). There are a number of promising applications in the areas of drug screening (Nakano et al. 2005), PCR amplification (Zhang et al. 2002), ultrasonic droplet imaging (Ferrara et al. 2007), and microbubble logic based on the implementation of Boolean algebra (Prakash and Gershenfeld 2007). Droplet microfluidics has been explored on the chip-based devices as well as on the centrifugal microfluidic platforms. For example, Haeberle et al. (2007b) utilized droplet generation on a disc for mixing liquids, and in another study, the same group has demonstrated alginate droplet formation on a rotating disc (Haeberle et al. 2007a). They (Haeberle et al. 2006) also presented a mechanism for digital droplet generation that could be achieved by alternating the direction of rotation. Another group (Chakraborty and Chakraborty 2010) demonstrated a mechanism for microbubble generation on a rotating disc. Recently, Schuler et al. (2015) demonstrated digital nucleic acid amplification based on generating droplets in oil and collecting them using buoyancy force. Both this method and the droplet generation method presented in this paper
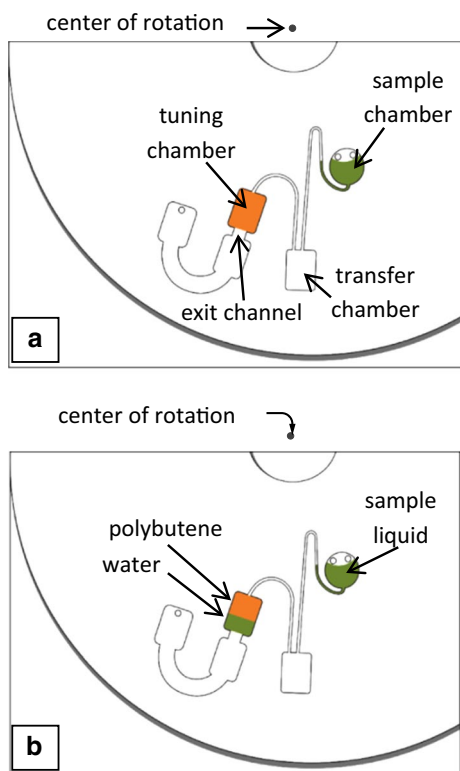
Fig. 1 a Schematic design of a tunable hydrophobic siphon valve. **b** Schematics of the liquid volume definition setup that utilizes a hydrophobic siphon. The volume of sample liquid transferred to the transfer chamber corresponds to the volume of liquid that empties from the tuning chamber

are different from earlier studies, since the carrier phase (oil is Schuler et al. study or polybutene in our study) is stationary.

Implementation of all the fluidic handling processes presented in this work, from tunable hydrophobic siphon valves and on-demand volume definition, to enhanced liquid heating by reduction in evaporation losses as well as droplet generation on discs, relies on the use of polybutene. At room temperature, polybutene is a viscous liquid polymer that is less dense than water. Commercial applications of this polymer include sealants, adhesive products, and cosmetics.

2 Concepts

Design and fluidic applications.

2.1 Tunable hydrophobic siphon and on-demand volume definition

The fluidic design consists of a sample liquid chamber, a transfer chamber, and a tuning chamber, all connected

through a ventless network of channels (Fig. 1a). The liquid in the tuning chamber is held in place by capillary forces due to the hydrophobicity of the exit channel, which functions as a passive hydrophobic valve. As the rotational frequency is increased, the centrifugal force applied to the liquid in the tuning chamber exceeds the restraining capillary forces and the liquid in the tuning chamber empties into a downstream chamber. During this step, an increase in the empty (non-filled) volume in the tuning chamber results in a pressure drop in the tuning chamber. This pressure drop (vacuum) causes the transfer of liquid from the sample chamber over the crest of the hydrophobic siphon and into the transfer chamber (see Fig. 1a).

This type of hydrophobic siphon valve can be tuned to open at different angular frequencies (initiating transfer of the sample liquid) depending on the density and height of the liquid in the tuning chamber. For example, for the same geometrical design, the valve (exit channel) of the tuning chamber filled with water bursts at a lower angular velocity compared to a case when the tuning chamber is filled with a liquid that has lower density, such as polybutene. Therefore, by selecting the height of the liquid column (i.e., liquid volume) and type of the liquid residing in the tuning chamber, the user can select the angular velocity at which the hydrophobic siphon will be activated.

The tunability of this type of hydrophobic siphon can also be used for on-demand liquid volume definition. This volume definition technique relies on utilization of a combination of immiscible liquids of different densities to fill the tuning chamber. It is important to use immiscible liquids in the tuning chamber (such as water and oil) that separate along a continuous interface. Polybutene has a lower density than water, and it is insoluble in water. For the liquid volume definition demonstrated in this work, we use water and polybutene as working liquids in the tuning chamber (Fig. 1b). The exit channel of the tuning chamber has a fixed width. Hence, the parameters that affect the burst angular velocity of this valve are the angular velocity, liquid density, and the radial position of each liquid column. If the angular velocity of the disc is selected to be above the burst angular velocity of the water, but below the burst angular velocity of the polybutene (less dense liquid), then the water will empty from the tuning chamber, but the polybutene will stay in the tuning chamber. Thus, a volume of the sample liquid equal to the volume of water ejected from the tuning chamber can be transferred from the sample chamber to the transfer chamber. It is important to note that the segment of the siphon channel that connects the bottom of the sample chamber to the siphon crest is a dead volume. Therefore, due to a very small dead volume of the sample, the volume of the sample transferred to a transfer chamber is slightly smaller than the volume of the emptied water. This difference is insignificant and does not need to
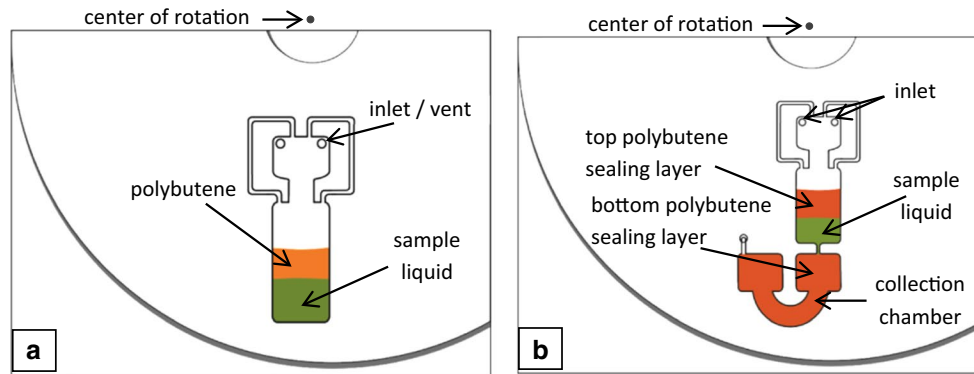
Fig. 2 **a** Schematic design of a sealed chamber for applications that require thermal cycling. In this design, the polybutene layer seals the sample liquid from the top. Polybutene is an appropriate choice of sealant since it is less dense than water; it is water insoluble and highly viscous. **b** Design schematic of sample liquid sandwiched in between polybutene. During thermal cycling, the liquid (e.g., PCR solution) is contained and sealed from both the top and bottom. After thermal cycling, the sample can be transferred out of the sample chamber to the collection chamber as an array of droplets

be taken into account while selecting the amount of water to be placed in the tuning chamber.

2.2 Sealing the chamber for efficient thermal cycling

In order to prevent evaporation of sample liquid and to increase heating efficiency during thermal cycling, we sealed a fluidic chamber with polybutene. Polybutene is highly viscous, and it is thermally stable within the required temperature range.

A fluidic network that has a rectangular chamber for holding both the sample liquid and polybutene (illustrated in Fig. 2a) was fabricated on the microfluidic disc. Since polybutene is less dense than water, it floats on the water.

The method used for heating the chamber in this design was contact heating. It is possible to apply an electrical potential across resistors on the spinning disc via an assembly of slip rings and contact brushes. The resistors are placed directly underneath the chambers, and when current passes through the resistors, the temperature of the resistors (and the chambers) rise up due to Joule heating. The advantage of heating a spinning disc is that the cooling portion of the thermal cycling can be simply effected via convective cooling (convective cooling is significantly more efficient compared to a stationary chip and the convective heat transfer coefficient, and thus the efficiency of cooling is increased with the angular velocity of the disc) (Bergman et al. 2011).

In cases where the sample liquid needs to be transferred to another chamber after thermal cycling, a sandwich design can be utilized (Fig. 2b). In this design, the sample liquid is sealed from both the top and the bottom. The two chambers are connected via a narrow channel, and by increasing the spin rate, the sample liquid can be ejected as droplets into the collection chamber. Since water is denser than polybutene, it can easily move to the bottom of the collection chamber and be separated for any process post-thermal cycling. This process can be utilized in DNA hybridization on microarrays after PCR (Wang and Li 2011). Water droplet generation with polybutene used as a stationary media is described in the next section.

2.3 Droplet generation

Researchers have demonstrated droplet generation on rotating discs for different applications such as microbead fabrication (Haeberle et al. 2007a), liquid mixing (Haeberle et al. 2007b), and liquid flow routing (Haeberle et al. 2006) where shear stress of the carrying liquid is used to pinch off a stream of liquid sample to generate droplets. The droplet generation technique on a rotating disc demonstrated in the present work does not require a stream of a liquid carrier phase for shearing and pinching off the water droplets. Instead the carrier phase is stationary, and droplets are formed by means of an unstable equilibrium between capillary forces, centrifugal forces, and buoyant forces acting on the sample liquid at the exit of the tuning chamber. The dynamics of droplet formation and pinch-off have been studied by several researchers (Wilkes et al. 1999; Chen et al. 2002; Ambravaneswaran et al. 2000; Shi et al. 1994). After a sample liquid droplet is formed at the exit of the channel, it grows until it separates and then another droplet starts to grow (Fig. 3). The stationary carrier phase has numerous advantages over the flowing shear phase: Smaller shear forces are applied to the sample liquid, and shear forces do not depend on the amount of remaining carrying media (since as the amount of the carrying media remaining in the reservoir is reduced, the shear stresses applied to the pinch-off region of the droplet are also reduced), the ability to produce a continuous stream of droplets for
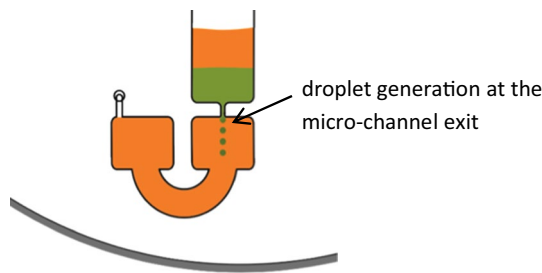
Fig. 3 Droplet generation in a stationary carrier phase on a rotating disc. The aqueous sample liquid droplets are dispensed into the stationary polybutene layer. The droplet formation is influenced by the unstable equilibrium between the centrifugal, capillary, and buoyant forces present at the interface between sample fluid and polybutene

a longer period of time, etc. It is also possible to use novel liquid handling steps in stationary carrying media. For example, the stationary carrier phase can be heated, and the droplets are also heated as they pass through the carrying phase. Since the carrying phase is stationary, it is easier to create a constant temperature profile required for such an application.

3 Analytical model

The sample liquid rising in the siphon experiences the centrifugal pressure that is given by:

$$dP_\omega = \rho \omega^2 r dr \tag{1}$$

Hence, the maximum hydrostatic pressure head on the sample liquid in the siphon is given by:

$$P_\omega = \rho \omega^2 \int_{R_1}^{R_2} rdr = \frac{\rho \omega^2}{2}\left(R_2^2 - R_1^2\right) \tag{2}$$

where ρ is the density of the sample liquid, ω is the angular velocity, and R_1 and R_2 are the radial positions of the top and bottom levels of the sample liquid, respectively (Fig. 4). Thus, the maximum pressure head will occur when there is no liquid left in the sample chamber and the siphon is completely filled (from the bottom of the sample liquid chamber to the crest of the siphon).

The expansion of volume due to emptying of the tuning liquid generates a pressure drop that is given by:

$$P_{neg} = P_{atm} \frac{V_{mid}}{V_{mid} + A_{tn}\Delta L} \tag{3}$$

where V_{mid} is the volume of the air trapped in the ventless space between the sample and tuning liquids, A_{tn} is the tuning chamber's cross-sectional area, and ΔL is the distance travelled by the top meniscus of the tuning liquid in the
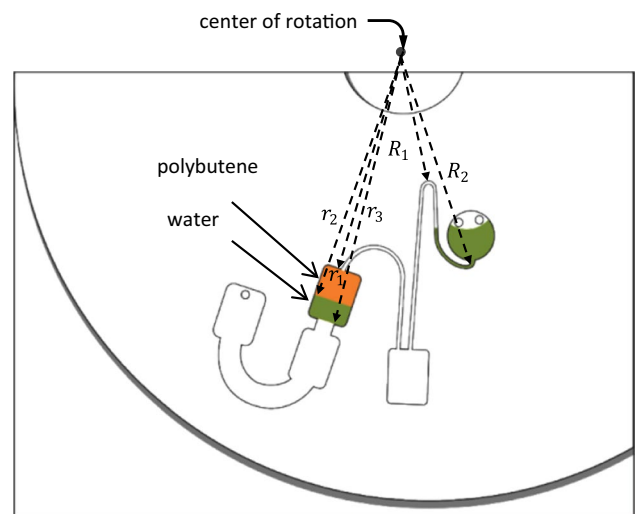
Fig. 4 Geometry of the tunable hydrophobic siphon

tuning chamber. This pressure drop counteracts the centrifugal pressure that is exerted on the sample liquid within the siphon; it is the driving force that pulls the sample liquid toward the center of the disc and activates the siphon. The maximum generated pressure drop is:

$$
\begin{aligned}
P_{neg(max)} &= P_{atm} \frac{V_{mid}}{V_{mid} + A_{tn}\Delta L_{max}} \\
&= P_{atm} \frac{V_{mid}}{V_{mid} + A_{tn}(r_3 - r_1)}
\end{aligned}
\tag{4}
$$

where r_1 and r_3 are the radial positions of the top and bottom of the tuning chamber, respectively (Fig. 4).

In our previous work (Soroori et al. 2014), we demonstrated that the maximum angular velocity to achieve a successful transfer of sample liquid in a hydrophobic siphon is given by:

$$\omega_{max} = \sqrt{\frac{2 \cdot P_{atm} \cdot A_{tn} \cdot (r_3 - r_1)}{\rho \cdot \left(R_2^2 - R_1^2\right) \cdot (V_{mid} + A_{tn}(r_3 - r_1))}} \tag{5}$$

Above this critical angular velocity, the hydrostatic pressure within the sample liquid overcomes the vacuum created within the tuning chamber with the working liquid and the sample liquid does not go over the crest of the siphon.

Within the tuning chamber (Fig. 4), the hydrostatic pressures at the bottoms of the several working liquids are [in accordance with Eq. (2)]:

$$P_{\omega,1} = \rho_1 \omega^2 \int_{r_1}^{r_2} rdr = \frac{\rho_1 \omega^2}{2}\left(r_2^2 - r_1^2\right) \tag{6}$$

$$P_{\omega,2} = \rho_2 \omega^2 \int_{r_2}^{r_3} rdr = \frac{\rho_2 \omega^2}{2}\left(r_3^2 - r_2^2\right) \tag{7}$$

where ρ_1 is the density of the lighter liquid (i.e., polybutene), ρ_2 is the density of the heavier liquid (i.e., water), ω is the angular velocity, and r is the radial position of the column of liquid. Combining Eqs. 6 and 7, we obtain for the total hydrostatic head at the exit of the tuning chamber:

$$P_{\omega,Tot} = \frac{\omega^2}{2}\left[(\rho_1 - \rho_2)r_2^2 - \rho_1 r_1^2 + \rho_2 r_3^2\right] \qquad (8)$$

The fluid meniscus at the tuning chamber's exit has a pressure given by (Chen et al. 2008):

$$\Delta P_b = \frac{2\gamma_{la}}{w}\left[-\frac{w}{h}\cos\theta_c - \cos(\theta_c + \beta)\right] \qquad (9)$$

where γ_{la} is the liquid–air surface tension, w and h are the hydrophobic (or capillary) channel width and height, respectively, θ_c is the fluid contact angle, and β is the expansion angle at the end of the capillary channel.

The burst angular velocity of the tuning chamber's exit capillary channel (hydrophobic valve) can be determined by balancing the capillary forces at the exit of the tuning chamber, the hydrostatic pressure head of the tuning liquid(s) (we assume that the tuning chamber is completely filled), and the subatmospheric pressure in the ventless network that also acts against the exit of the tuning liquid(s):

$$\Delta P_b + \left(P_{atm} - P_{neg}\right) = P_{\omega,Tot} \qquad (10)$$

Therefore, the minimum burst angular velocity for this hydrophobic valve (when $\Delta L = 0$) is given by:

$$\omega_{min} = 2\sqrt{\frac{\frac{\gamma_{la}}{w}\left[-\frac{w}{h}\cos\theta_c - \cos(\theta_c + \beta)\right]}{(\rho_1 - \rho_2)r_2^2 - \rho_1 r_1^2 + \rho_2 r_3^2}} \qquad (11)$$

For the case where the tuning chamber is filled only with one type of liquid, the minimum burst angular velocity is given by:

$$\omega_{min} = 2\sqrt{\frac{\frac{\gamma_{la}}{w}\left[-\frac{w}{h}\cos\theta_c - \cos(\theta_c + \beta)\right]}{\rho(r_3^2 - r_1^2)}} \qquad (12)$$

4 Experimental

The microfluidic discs were made from plastics by using rapid prototyping techniques. Each disc was composed of five layers: three 1.5-mm-thick clear acrylic layers and two 75-μm-thick double-sided pressure-sensitive adhesive (PSA) layers. The PSA layers were sandwiched between the acrylic layers; the top and bottom layers of the disc were made of acrylic. Acrylic sheets (McMaster-Carr, USA) were cut by a CO_2 laser cutter (Universal Laser Systems, USA), and the PSA layers (Flexcon, USA) were cut by a standard cutter-plotter (Graphtec America, Japan). The fluidic features were designed using computer-aided design (CAD) software, and the drawing files were used

as the input for cutting hardware such as the laser cutter. More details on the microfluidic disc fabrication strategy employed by our team can be found in the paper published by (Siegrist et al. 2010). In the custom built system (CD Imager K1000, Key Lead Solutions Inc., USA), the spinner motor was integrated with an image acquisition platform comprising a strobe light, camera, and a stereomicroscope all controlled through a graphical user interface. The CD Imager system is identical to what we used in our previous project (Soroori et al. 2014).

The resistive heating method was used for experiments that required heating the sample liquid. Resistors (10 Ω, 25 W, Bourns, USA) were mounted on a printed circuit board (PCB) and placed directly underneath the fluidic chambers on the disc. Each resistor was placed in direct contact with the bottom of its corresponding fluidic chamber. As electrical potential was increased, more Joule heat was generated and it was transferred via heat conduction to the liquid in the chamber. Both the PCB and microfluidic disc were mounted on a slip ring assembly connected to the electronic controls via metal brushes. More details about the slip ring assembly can be found in the earlier paper published by our group (Martinez-Duarte et al. 2010).

The liquid polymer used in our experiments was PB24 polybutene (Soltex, USA). Both clear and colored PB24 polymers were used for the applications demonstrated in this paper.

5 Results and discussion

5.1 Tunable hydrophobic siphon valve

In order to demonstrate the concept of tuning a hydrophobic siphon valve, three different types of liquids with different densities were used: polybutene ($\rho = 888$ kg/m³), water ($\rho = 1000$ kg/m³), and salt water ($\rho = 1031$ kg/m³). According to Eq. 12, it was expected that polybutene, which has the lowest density, would require the highest angular velocity of the disc to burst the tuning chamber's hydrophobic valve. The process of emptying the tuning chamber and transferring the sample liquid via the hydrophobic siphon to the transfer chamber is shown in Fig. 5.

The theoretical and experimental burst angular velocities were compared for the three liquids tested and are summarized in Fig. 6. The chamber geometry and the height of the tuning fluid were the same for all three experiments. Table 1 shows the values of parameters used for theoretical calculations.

Based on Eqs. 5 and 12, there is a range of angular velocities within which the hydrophobic siphon can be activated. The results presented by the bar graphs in Fig. 6 indicate the minimum angular velocity for this system to be
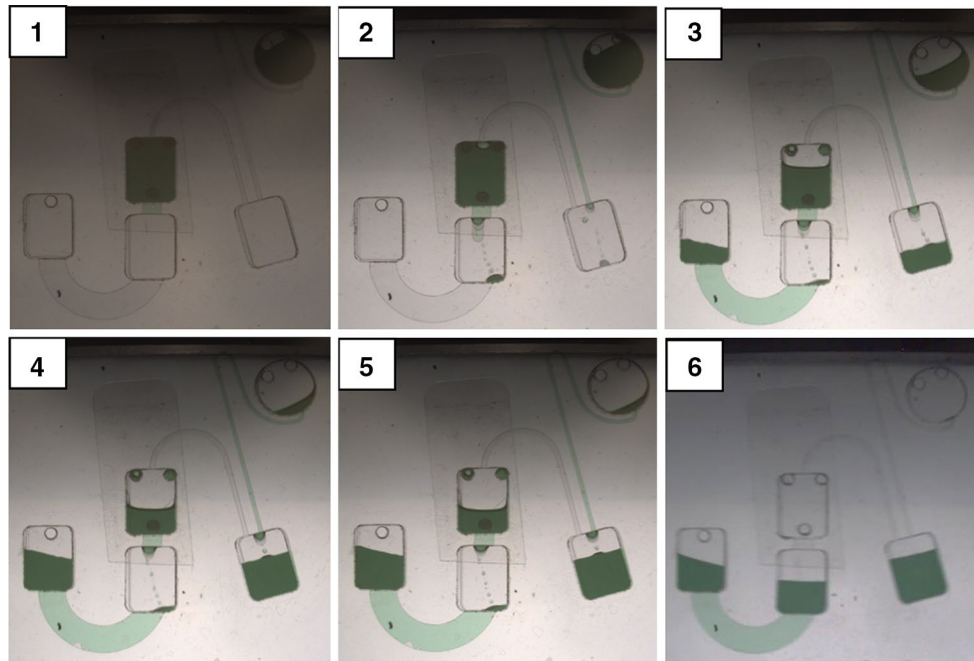
Fig. 5 Process of emptying working liquid (water) from the tuning chamber induces the transfer of the sample liquid into the transfer chamber. Sequence of the captured images includes a stationary disc (1), bursting the tuning valve (2), gradual transfer of the sample liquid (3–5), leading to the complete transfer of the sample liquid into the transfer chamber (6)
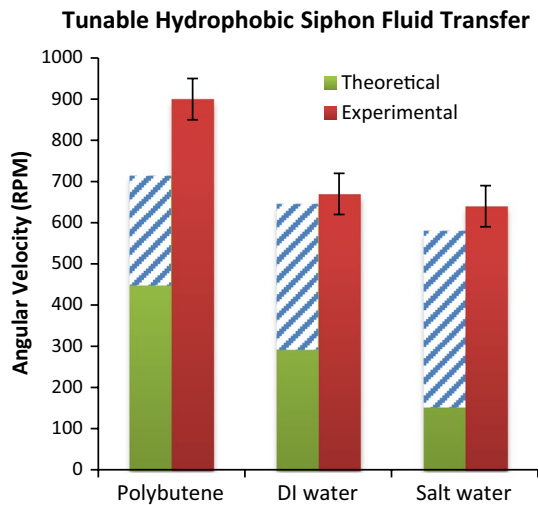
Fig. 6 Minimum angular velocity at which the liquid begins to exit the tuning chamber. The *plot* shows a trend that as the tuning liquid becomes heavier, the hydrophobic siphon can be activated at lower angular velocities. The error bars for experimental values indicate $\pm$ 50 RPM due to 50 RPM increments in changing the angular velocity. The hashed areas in the column of theoretical values of tuning valve's burst angular velocity indicate a range of 30° for liquid contact angle (representing the increase in the contact angle from smooth to rough plastic). The experimental values are based on 5

operational (exit of the tuning liquid from the tuning chamber with the subsequent sample liquid transfer) for each liquid. Somewhat higher experimental results for water

are likely due to some stretching of the air pocket in the ventless space and air diffusion through the tuning liquid. The biggest difference between the theoretical prediction and experimental results is for polybutene. Polybutene is a non-Newtonian fluid with the propensity to adhere strongly to materials such as polymer plastics (James 2009). The viscous and elastic properties of polybutene and its adhesion to channel walls cause fluid behavior that deviates from the classical fluid mechanics theory (Benedek 2004). The flow of polybutene is similar to the stretching of honey; hence, a higher centrifugal force (i.e., higher angular velocity) is required to push such liquid out of the tuning chamber.

The hashed areas on the theoretical values represent uncertainty in liquid contact angles within fluidic channels. Researchers have shown that contact angles of water on plastic can increase by about 30° in microchannels with significant surface roughness (Saarikoski et al. 2009). It is also very difficult to measure the liquid contact angle inside channels though some researchers have used a tensiometer to measure liquid contact angle inside polycarbonate capillary channels (Extrand and Moon 2014) since only stationary and not advancing contact angle measurements are possible. We have accounted for the uncertainty of contact angle values within machined microchannels by including a range of 30°—from contact angle of the liquid on smooth to that on very rough plastic.

Table 1 Parameters used for calculation of theoretical burst angular velocity

	Density (ρ)—kg/m^3	Surface tension (γ_{la})—N/m	Contact angle (θ_c)—Deg°
Polybutene	888	0.065	105 (lowest), 135 (highest)
DI water	1000	0.073	95 (lowest), 125 (highest)
Salt water	1031	0.070	90 (lowest), 120 (highest)

Other parameters used for calculating the theoretical value include: $\beta = 90°$, $r_1 = 33$ mm, $r_3 = 41$ mm, $w = 2$ mm, and $h = 75$ μm
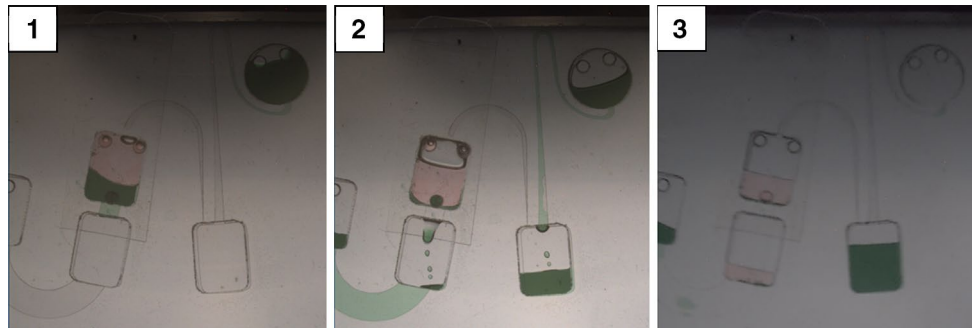
Fig. 7 Multistage volume definition using water and polybutene as tuning liquids. The sequence of fluidic steps includes: a stationary disc with water (*green* due to added dye) at the bottom of the tuning chamber as well as a sample liquid, polybutene (*pink color*), used as a second tuning liquid (1); water empties completely from the tuning chamber, bringing about the transfer of the corresponding volume of the sample liquid from the sample chamber into the transfer chamber (2), and the transfer of the remaining sample liquid into the transfer chamber by emptying the polybutene from the tuning chamber (3) (color figure online)

5.2 On-demand volume definition of liquid

The tuning chamber can also be used for an on-demand volume definition of liquid since for any volume of the tuning liquid that empties from the tuning chamber, there is a corresponding volume of the sample liquid that is transferred to the transfer chamber. In a perfectly sealed system, the volume of the emptied tuning liquid is equal to the volume of the sample liquid transferred minus the dead volume between the bottom of the sample chamber and the crest of the siphon. It is important to note that in order to achieve a reliable multistage on-demand volume definition, it is necessary to use several layers of non-miscible tuning liquids with different densities in the tuning chamber. For our proof-of-concept design, we used water and polybutene as tuning liquids. Different proportions of these liquids determine the amount of sample liquid that can be selectively transferred to the transfer chamber. The denser liquid empties first at a lower angular velocity, and the lighter liquid can be emptied as soon as a high enough angular velocity is achieved. For many multistep biological and chemical assays such as sample preparation and DNA hybridization on microarrays, specific volumes of sample liquids or reagents are required to be mixed in different chambers at various points. The on-demand multistage volume definition technique presented in this work can significantly simplify the fluidic designs and enhance the efficiency of liquid flow control on microfluidic discs. The process of a multistage volume definition is demonstrated in Fig. 7.

Three different ratios of polybutene to water in the tuning chamber were used to study the effect of variation in the proportion of tuning liquids. Different tuning liquid volumes resulted in different liquid column heights in the tuning chamber. The change in the heights of the liquids (i.e., radial position of their top menisci) affects the value of the burst angular velocity of the tuning valve (see Eq. 11). The theoretical and experimental results are summarized in Fig. 8.

As discussed above, the observed deviation of polybutene's experimentally observed burst angular velocity value that is higher than its theoretical prediction relates to the fact that polybutene is a non-Newtonian fluid. As the amount of polybutene in the tuning liquid mix decreases, the theoretical prediction of angular velocity at which the sample liquid is transferred becomes closer to the experimental values. This behavior of polybutene has a positive effect since while polybutene-to-water ratio change would not have a great effect if polybutene were a Newtonian fluid (see the blue bars in Fig. 8), due to non-Newtonian nature of polybutene, change in the polybutene-to-water ratio in the tuning chamber does affect the burst velocity significantly (as evidenced by the red bars in Fig. 8). Since theoretical predictions of polybutene's behavior are not
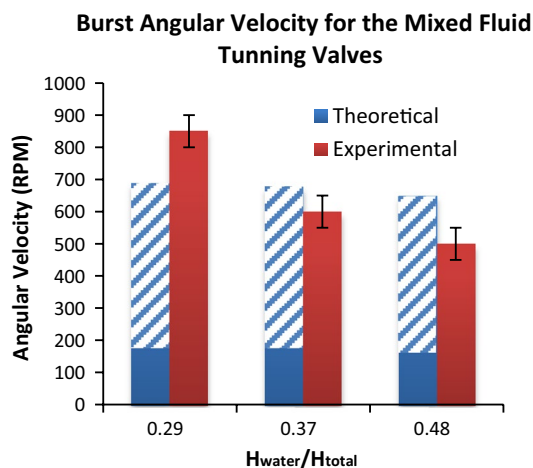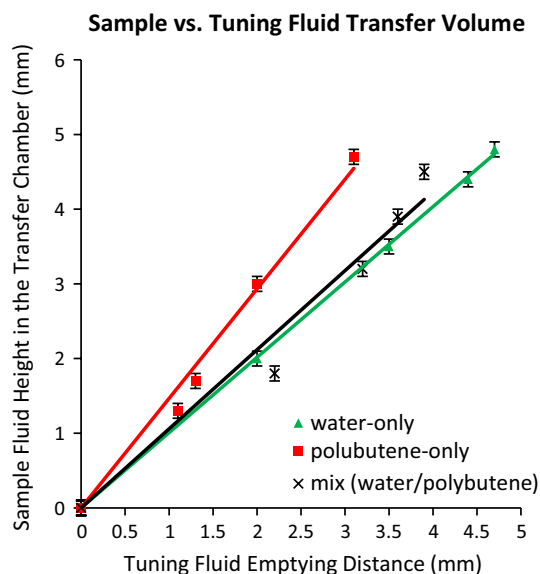
Fig. 8 Theoretical (*blue*) versus experimental (*red*) angular velocity at which the valve of the tuning chamber bursts open for different ratios of polybutene to water (expressed in ratio of liquid columns' heights). The water (denser liquid) is the liquid in contact with the exit valve. As expected, as the amount of water increases (ratio of polybutene to water decreases) the tuning chamber valve bursts at lower angular velocities. The error bars for experimental values indicate $\pm$ 50 RPM since the angular velocity was changed in 50 RPM increments. The *hashed areas* on the *bars* representing theoretical values of the tuning valve's burst angular velocity indicate a range of 30° for liquid contact angle (representing the increase in the contact angle from smooth to rough plastic). The experimental values are based on 5 measurements. Values used for theoretical calculations (Eq. 11) from left to right were 38.1, 37.8, and 37.2 mm (color figure online)


Fig. 9 Volume of the sample liquid transferred into the transfer chamber versus volume of tuning liquid emptied from the tuning chamber. Since the tuning and transfer chambers had an identical cross-sectional area, the change in level of liquid would directly relate to the volume of the liquid that was transferred. The linear trend lines are plotted for comparison. Water-only scenario demonstrated nearly a one-to-one correspondence between the volume of the tuning liquid emptied and the volume of the sample liquid transferred. The *error bars* show $\pm$ 0.1 mm uncertainty in measuring advancement of liquid meniscus

possible, fluidics design should rely on empirical validation whenever polybutene is used.

The theoretical calculations presented in Figs. 6 and 8 are associated with a wide range of uncertainty due to variation in fluid contact angle (30° range) that is used in these calculations. The comparison of the theoretical prediction and experimental observation demonstrates the consistency of the theoretical model with the observed behavior. The hashed areas on the theoretical values of angular velocity represent the range of possible values associated with different contact angle values (since it was impossible to measure the contact angle inside microchannels).

In order to correlate the volume of the sample liquid transferred into the transfer reservoir with the volume of the tuning liquid exiting the tuning chamber, an experimental study was performed for three scenarios. In the first scenario the tuning chamber was completely filled with water, in the second the tuning chamber was completely filled with polybutene, and in the third scenario a mix of water and polybutene was used in the tuning chamber. The experimental results are presented in Fig. 9.

The study has demonstrated that when the tuning chamber is completely filled with water, there is almost a one-to-one correspondence between the volume of tuning liquid that is emptied and the volume of the sample liquid that is

transferred to the transfer reservoir (the dead volume in the siphon leads to a small difference between the corresponding volumes). In contrast, when polybutene is used, this one-to-one correspondence between volumes is not maintained—more sample liquid is transferred than the volume of the polybutene that is emptied from the tuning chamber. This behavior is due to the elasticity of polybutene. This elastic behavior of polybutene also causes a delay in sample liquid transfer as compared to the scenario when only water is used in the tuning chamber (see supplementary video).
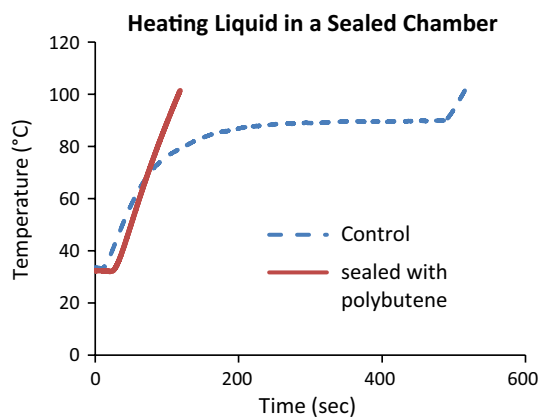
5.3 Temperature measurements of chambers sealed with polybutene

The utility of polybutene as a sealing layer for heating of a sample was also tested. The polybutene was placed on top of the sample in the test chamber, and upon spinning the disc, the layer of polybutene stays on top of the sample liquid (water) since polybutene's density is lower than that of the water. Temperature measurements were taken to study the effectiveness of the polybutene seal. One set of temperature measurements was taken for a solution with no sealing layer (control), and another set of measurements was taken when the same volume
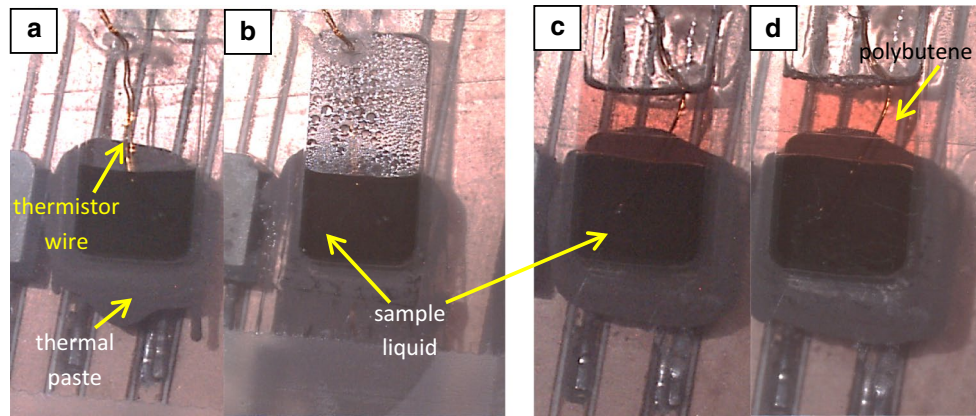
Fig. 10 Contact heating of fluidic chambers with resistors placed directly underneath the chambers. Images demonstrate: **a** the control (no sealing layer) before heating, **b** the control after heating, **c** the water sealed with polybutene before heat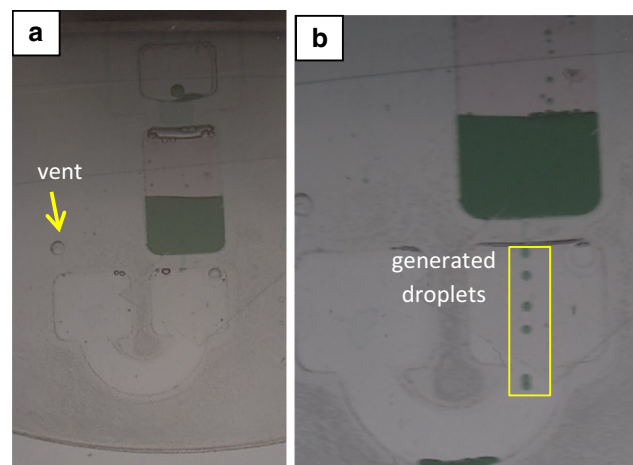ing, and **d** the water sealed with polybutene after heating. Difference between images **b** and **d** demonstrates the effectiveness of the polybutene as a sealing layer in preventing undesired evaporation

Fig. 11 Contact heating of fluidic chambers with resistors placed underneath the chambers. The sealed chamber with polybutene shows a much faster heating rate (about 5 times faster) for reaching 100 °C. Error in temperature measurement by the thermistor is ±3 %

Fig. 12 Sandwich design to seal the sample liquid for heating. **a** The sample liquid (*green*) is sealed from the top by polybutene (*light red*) and the bottom by a chamber filled with polybutene (clear) connected via a microchannel. This design is used for cases that require sample liquid transfer to another chamber after thermal cycling. **b** Droplets are generated and collected in the stationary polybutene as the sample liquid exits into the lower chamber through the microchannel as the spin rate of the disc is increased (color figure online)

5.4 Sealed chamber (sandwich design) and droplet generation

Finally a layer of polybutene can also be used as a stationary phase for droplet fluidic applications. It is possible to employ polybutene for multiple purposes on the same disc, simplifying the disc design. For example, polybutene can be used both as a sealing layer to prevent evaporation in PCR amplification and as a stationary phase for droplet generation. For the cases that require sample liquid transfer to another chamber after thermal cycling, a sandwich

of water was covered by a layer of polybutene (see Fig. 10). The maximum target temperature was about 100 °C (approximate upper level for thermal cycling applications such as PCR amplification). The feedback loop between the thermistor and temperature controller was established to achieve 100 °C. In realistic PCR amplification, the actual heating rate will be slower in the vicinity of the target temperature in order not to overshoot the target temperature.

The temperature measurements for the open (control) and sealed chambers indicated that the sealed chamber could be heated to about 100 °C in about 100 s and it took about 500 s for the open chamber to reach that temperature (Fig. 11). Both sets of measurements were taken, while the disc was spinning at 700 RPM.

design can be used for sealing. In this design, the sample liquid is sealed from the top and the bottom by polybutene layers. The bottom polybutene layer is located in a separate reservoir connected to the sample reservoir by a microchannel to prevent mixing of the lighter polybutene and heavier water (Fig. 12a). The inlet access holes are sealed, and the only vent is at the left side of the U-shaped chamber. After finishing the thermal cycling, the sample liquid can be transferred out of the sealed chamber by increasing the spin rate and ejecting the sample liquid as droplets (Fig. 12b).

This mechanism for forming droplets on a rotating disc using a stationary phase (rather than a moving carrier phase to shear off droplets) has not been demonstrated before in the literature. It has a number of advantages listed in Sect. 2.3 above. Multiple arrays of droplets may be generated from the same reservoir through parallel microchannels, and this type of multiplexing is much easier to implement with the current design than with streams of shearing carrier liquids.

6 Conclusions

In this article, we demonstrated several applications of polybutene in microfluidic discs. In one application, polybutene was used as a tuning liquid within a system comprising a tuning reservoir connected through a ventless network to a sample reservoir. The transfer of the sample liquid into a transfer reservoir was triggered by the exit of the tuning liquid through a capillary valve. Adjusting the volume of the polybutene in the tuning chamber, we can tune the burst angular velocity of the tuning valve and thus control the activation of the transfer of the sample liquid.

In another application, we demonstrated on-demand volume definition of a liquid. If a combination of several immiscible tuning liquids with different densities is placed in the tuning chamber, the heavier liquid (in this case water) will stay at the bottom of the chamber and it exits the tuning chamber at a lower angular velocity compared to the lighter liquid (i.e., polybutene). Different burst angular velocities for the two tuning liquids ensure that the sample liquid can be transferred in several fractions as corresponding tuning liquids exit the tuning reservoir in succession. Hence, the sample liquid volume definition can be performed "on-demand" and in multiple stages (in this case two independent steps). The transferred volume of the sample liquid corresponds to the volume of liquid that exits the tuning chamber.

Polybutene can also be used as sealing layer on top (and possibly on the bottom) of the sample liquid to enhance heating efficiency and reduce unwanted evaporation of the sample liquid during thermal cycling. In our experiments, we used polybutene as a sealing layer for the sample liquid

(water) and demonstrated fivefold increase in the heating rate as compared to the equivalent test setup without sealing layer. Besides improvement in speed of thermal cycling, additional biocompatibility and PCR inhibition studies should be performed before the demonstrated technology can be implemented for PCR amplification.

Finally, a sandwich seal design has been demonstrated that can be used to not only seal but also transfer the sample liquid after thermal cycling. In this design, the sample liquid is sealed from both the top and bottom and it can be transferred to another chamber by increasing the spin rate and having sample liquid be ejected as droplets. As an alternative to other droplet formation mechanisms on microfluidic discs, this method does not rely on intersecting streams of carrier phase (such as oil). In the demonstrated application, the carrier phase is stationary. It has number of advantages over the moving carrier phase implementation such as smaller shear forces, independence of shearing forces on the remaining volume of the shearing liquid, ability to produce a continuous stream of droplets for prolonged period of time, and the ease of multiplexing to produce parallel arrays of droplets. In a recent work, similar type of stationary carrier phase has been demonstrated by Schuler et al. In this method, the droplets are formed through a nozzle; however, they travel to top of the oil (carrier phase) driven by buoyancy force and accumulating as droplets. The benefit of using polybutene is in possible integration of this liquid polymer when used with other fluidic functions such as volume definition and sealing for more efficient heating.

The polybutene-based fluidic techniques for valving, volume definition, and enhanced thermal cycling demonstrated in this work have potential for use in developing streamlined and robust biological or chemical assays on discs.

References

Abi-Samra K, Clime L, Kong L, Gorkin R, Kim T-H, Cho Y-K, Madou M (2011a) Thermo-pneumatic pumping in centrifugal microfluidic platforms. Microfluid Nanofluidics 11(5):643–652. doi:10.1007/s10404-011-0830-5

Abi-Samra K, Hanson R, Madou M, Gorkin RA III (2011b) Infrared controlled waxes for liquid handling and storage on a CD-microfluidic platform. Lab Chip 11(4):723–726

Aeinehvand MM, Ibrahim F, Harun SW, Djordjevic I, Hosseini S, Rothan HA, Yusof R, Madou MJ (2015) Biosensing enhancement of dengue virus using microballoon mixers on centrifugal microfluidic platforms. Biosens Bioelectron 67:424–430

Al-Faqheri W, Ibrahim F, Thio THG, Bahari N, Arof H, Rothan HA, Yusof R, Madou M (2015) Development of a passive liquid valve (PLV) utilizing a pressure equilibrium phenomenon on the centrifugal microfluidic platform. Sensors 15(3):4658–4676

Amasia M (2011) Vapor-tight Ice valving in centrifugal microfluidics for PCR applications. In: Proceedings of micro-total analysis systems

Amasia M, Cozzens M, Madou MJ (2012) Centrifugal microfluidic platform for rapid PCR amplification using integrated thermoelectric heating and ice-valving. Sens Actuators B Chem 161:1191–1197. doi:10.1016/j.snb.2011.11.080

Ambravaneswaran B, Phillips SD, Basaran OA (2000) Theoretical analysis of a dripping faucet. Phys Rev Lett 85(25):5332

Beaulieu I, Geissler M, Mauzeroll J (2009) Oxygen plasma treatment of polystyrene and Zeonor: substrates for adhesion of patterned cells. Langmuir 25(12):7169–7176

Benedek I (2004) Pressure-sensitive adhesives and applications. CRC Press, Boca Raton

Bergman TL, Lavine AS, Incropera FP, Dewitt DP (2011) Fundamentals of heat and mass transfer. Wiley, New York

Chakraborty D, Chakraborty S (2010) Controlled microbubble generation on a compact disk. Appl Phys Lett 97:234103. doi:10.1063/1.3524518

Chen AU, Notz PK, Basaran OA (2002) Computational and experimental analysis of pinch-off and scaling. Phys Rev Lett 88(17):174501

Chen JM, Huang P-C, Lin M-G (2008) Analysis and experiment of capillary valves for microfluidics on a rotating disk. Microfluid Nanofluidics 4(5):427–437

Clime L, Brassard D, Geissler M, Veres T (2015) Active pneumatic control of centrifugal microfluidic flows for lab-on-a-chip applications. Lab Chip 15(11):2400–2411

Czilwik G, Messinger T, Strohmeier O, Wadle S, von Stetten F, Paust N, Roth G, Zengerle R, Saarinen P, Niittymäki J (2015a) Rapid and fully automated bacterial pathogen detection on a centrifugal-microfluidic LabDisk using highly sensitive nested PCR with integrated sample preparation. Lab Chip 15(18):3749–3759

Czilwik G, Schwarz I, Keller M, Wadle S, Zehnle S, von Stetten F, Mark D, Zengerle R, Paust N (2015b) Microfluidic vapor-diffusion barrier for pressure reduction in fully closed PCR modules. Lab Chip 15(4):1084–1091

Dimov N, Clancy E, Gaughran J, Boyle D, Mc Auley D, Glynn MT, Dwyer RM, Coughlan H, Barry T, Barrett LM (2014) Solvent-selective routing for centrifugally automated solid-phase purification of RNA. Microfluid Nanofluidics 18(5–6):859–871

Ducree J, Haeberle S, Lutz S, Pausch S, von Stetten F, Zengerle R (2007) The centrifugal microfluidic bio-disk platform. J Micromech Microeng 17(7):S103–S115. doi:10.1088/0960-1317/17/7/S07

Extrand C, Moon SI (2014) Measuring contact angles inside of capillary tubes with a tensiometer. J Colloid Interface Sci 431:200–203

Ferrara K, Pollard R, Borden M (2007) Ultrasound microbubble contrast agents: fundamentals and application to gene and drug delivery. Annu Rev Biomed Eng 9:415–447

Gorkin R, Park J, Siegrist J, Amasia M, Lee BS, Park JM, Kim J, Kim H, Madou M, Cho YK (2010) Centrifugal microfluidics for biomedical applications. Lab Chip 10(14):1758–1773. doi:10.1039/B924109d

Gorkin R, Soroori S, Southard W, Clime L, Veres T, Kido H, Kulinsky L, Madou M (2011) Suction-enhanced siphon valves for centrifugal microfluidic platforms. Microfluid Nanofluidics. doi:10.1007/s10404-011-0878-2

Gorkin R III, Nwankire CE, Gaughran J, Zhang X, Donohoe GG, Rook M, O'Kennedy R, Ducrée J (2012a) Centrifugo-pneumatic valving utilizing dissolvable films. Lab Chip 12(16):2894–2902

Gorkin R, Nwankire CE, Gaughran J, Zhang X, Donohoe GG, Rook M, O'Kennedy R, Ducrée J (2012b) Centrifugo-pneumatic valving utilizing dissolvable films. Lab Chip 12:2894–2902. doi:10.1039/c2lc20973j

Haeberle S, Naegele L, Zengerle R, Ducrée J (2006) A digital centrifugal droplet-switch for routing of liquids. In: Proceedings of 10th international conference on miniaturized systems for chemistry and life sciences (μTAS2006)(Tokyo, Japan, 5–9 Nov), pp 570–572

Haeberle S, Naegele L, Burger R, Zengerle R, Ducrée J (2007a) Alginate micro-bead fabrication on a centrifugal microfluidics platform. In: MEMS

Haeberle S, Zengerle R, Ducrée J (2007b) Centrifugal generation and manipulation of droplet emulsions. Microfluid Nanofluidics 3(1):65–75. doi:10.1007/s10404-006-0106-7

Imaad SM, Lord N, Kulsharova G, Liu GL (2011) Microparticle and cell counting with digital microfluidic compact disc using standard CD drive. Lab Chip 11(8):1448–1456. doi:10.1039/C0lc00451k

James DF (2009) Boger fluids. Annu Rev Fluid Mech 41:129–142

Kim TH, Sunkara V, Abi-Samra K, Amasia M, Oh S, Kim N, Kim J, Kim H, Madou M, Cho YK (2011) Fully integrated centrifugal microfluidic platform for electrochemical biomarker detection. In: MicroTAS 2011 proceedings: miniaturized systems for chemistry and life sciences: 1668–1670

Madou M, Zoval J, Jia GY, Kido H, Kim J, Kim N (2006) Lab on a CD. Annu Rev Biomed Eng 8:601–628. doi:10.1146/annurev.bioeng.8.061505.095758

Martinez-Duarte R, Gorkin RA, Abi-Samra K, Madou MJ (2010) The integration of 3D carbon-electrode dielectrophoresis on a CD-like centrifugal microfluidic platform. Lab Chip 10(8):1030–1043. doi:10.1039/B925456k

Nakano M, Nakai N, Kurita H, Komatsu J, Takashima K, Katsura S, Mizuno A (2005) Single-molecule reverse transcription polymerase chain reaction using water-in-oil emulsion. J Biosci Bioeng 99(3):293–295

Oh SJ, Park BH, Jung JH, Choi G, Lee DC, Seo TS (2015) Centrifugal loop-mediated isothermal amplification microdevice for rapid, multiplex and colorimetric foodborne pathogen detection. Biosens Bioelectron 75:293–300

Park J-M, Cho Y-K, Lee B-S, Lee J-G, Ko C (2007) Multifunctional microvalves control by optical illumination on nanoheaters and its application in centrifugal microfluidic devices. Lab Chip 7:557–564. doi:10.1039/b616112j

Prakash M, Gershenfeld N (2007) Microfluidic bubble logic. Science 315(5813):832–835

Saarikoski I, Suvanto M, Pakkanen TA (2009) Modification of polycarbonate surface properties by nano-, micro-, and hierarchical micro–nanostructuring. Appl Surf Sci 255(22):9000–9005

Schuler F, Schwemmer F, Trotter M, Wadle S, Zengerle R, von Stetten F, Paust N (2015) Centrifugal step emulsification applied for absolute quantification of nucleic acids by digital droplet RPA. Lab Chip 15:2759–2766

Schwemmer F, Zehnle S, Mark D, von Stetten F, Zengerle R, Paust N (2015) A microfluidic timer for timed valving and pumping in centrifugal microfluidics. Lab Chip 15(6):1545–1553

Shi X, Brenner MP, Nagel SR (1994) A cascade of structure in a drop falling from a faucet. SCIENCE-NEW YORK THEN WASHINGTON: 219–219

Siegrist J, Gorkin R, Clime L, Roy E, Peytavi R, Kido H, Bergeron M, Veres T, Madou M (2010) Serial siphon valving for centrifugal microfluidic platforms. Microfluid Nanofluidics 9(1):55–63. doi:10.1007/s10404-009-0523-5

Soroori S, Kulinsky L, Kido H, Madou M (2014) Design and implementation of fluidic micro-pulleys for flow control on centrifugal microfluidic platforms. Microfluid Nanofluid 16(6):1117–1129

Steigert J, Grumann M, Brenner T, Riegger L, Harter J, Zengerle R, Ducrée J (2006) Fully integrated whole blood testing by real-time absorption measurement on a centrifugal platform. Lab Chip 6:1040–1044. doi:10.1039/b607051p

Strohmeier O, Keller M, Schwemmer F, Zehnle S, Mark D, von Stetten F, Zengerle R, Paust N (2015) Centrifugal microfluidic platforms: advanced unit operations and applications. Chem Soc Rev 44(17):6187–6229

Sundberg SO, Wittwer CT, Gao C, Gale BK (2010) Spinning disk platform for microfluidic digital polymerase chain reaction. Anal Chem 82:1546–1550. doi:10.1021/ac902398c

Teh S-Y, Lin R, Hung L-H, Lee AP (2008) Droplet microfluidics. Lab Chip 8(2):198–220

Thio THG, Soroori S, Ibrahim F, Al-Faqheri W, Soin N, Kulinsky L, Madou M (2013) Theoretical development and critical analysis of burst frequency equations for passive valves on centrifugal microfluidic platforms. Med Biol Eng Comput 51(5):525–535

van Oordt T, Barb Y, Smetana J, Zengerle R, von Stetten F (2013) Miniature stick-packaging–an industrial technology for pre-storage and release of reagents in lab-on-a-chip systems. Lab Chip 13:2888–2892

Wang L, Li PC (2011) Microfluidic DNA microarray analysis: a review. Anal Chim Acta 687(1):12–27

Wang G, Ho H, Chen Q, Yang K-L, Kwok H-C, Wu SY, Kong S-K, Kwan Y, Zhang X (2013) A lab-in-a-droplet bioassay strategy for centrifugal microfluidics with density difference pumping, power to disc and bidirectional flow control. Lab Chip 13:3698–3706

Wilkes ED, Phillips SD, Basaran OA (1999) Computational and experimental analysis of dynamics of drop formation. Phys Fluids 11(12):3577–3598

Zhang T, Chakrabarty K, Fair R (2002) System performance evaluation with system C for two PCR microelectrofluidic systems. In: Technical proceedings 2002 international conference on modeling and simulation of microsystems (San Juan, Puerto Rico, USA, 22–25 April), pp 48–53